# Mechanotransduction events at the physiological site of touch detection

Luke H. Ziolkowski[1], Elena O. Gracheva[1,2,3,4]*, Sviatoslav N. Bagriantsev[1]*

[1]Department of Cellular and Molecular Physiology, Yale University School of Medicine, New Haven, CT 06510, USA.

[2]Department of Neuroscience, Yale University School of Medicine, New Haven, CT 06510, USA.

[3]Program in Cellular Neuroscience, Neurodegeneration and Repair, Yale University School of Medicine, New Haven, CT 06510, USA.

[4]Kavli Institute for Neuroscience, Yale University School of Medicine, New Haven, CT 06510, USA.

*Correspondence to: elena.gracheva@yale.edu and slav.bagriantsev@yale.edu

**Abstract**

Afferents of peripheral mechanoreceptors innervate the skin of vertebrates, where they detect physical touch via mechanically gated ion channels (mechanotransducers). While the afferent terminal is generally understood to be the primary site of mechanotransduction, the functional properties of mechanically activated (MA) ionic current generated by mechanotransducers at this location remain obscure. Here, we report patch-clamp recordings from the afferent terminal innervating Grandry (Meissner) corpuscles in the bill skin of a tactile specialist duck. We show that mechanical stimulation evokes MA current in the afferent with fast kinetics of activation and inactivation during the dynamic phases of the mechanical stimulus. These responses trigger rapidly adapting firing in the afferent detected at the terminal and in the afferent fiber outside of the corpuscle. Our findings elucidate the initial electrogenic events of touch detection in the mechanoreceptor nerve terminal.

**Introduction**

In vertebrates, extrinsic touch is detected in the skin by cutaneous mechanoreceptors, somatosensory neurons of the peripheral nervous system. The afferent nerve fibers of these cells innervate the skin, where they form specialized ending structures which sense mechanical stimuli. Within the afferent terminals, mechanically-gated ion channels (mechanotransducers), such as Piezo2, detect touch and transform it into mechanically activated (MA) current (Handler and Ginty, 2021). Extracellular recordings of mechanoreceptor afferents have previously revealed voltage changes originating from the terminals in response to mechanical stimulation, but the intracellular dynamics of these signals are not understood (Loewenstein et al., 1958). As a result, direct evidence of mechanotransduction and MA current in the nerve endings of mechanoreceptors is lacking.

Studies of MA current and mechanotransducer biophysics have been limited to heterologous expression systems and dissociated somatosensory neurons *in vitro* (Coste et al., 2010; Lewis et al., 2017; Schneider et al., 2017; Zheng et al., 2019). Most notably, Piezo2, which mediates the detection of touch, displays fast-inactivating MA current in cultured cells and in dissociated neurons (Buchholtz et al., 2021; Chesler et al., 2016; Coste et al., 2010; Ranade et al., 2014; Wang et al., 2019). However, it is unclear whether electrophysiological responses of somas from dissociated neurons accurately reflect that of MA current in the afferent terminal, due to potential differences in membrane geometry, level of ion channel expression, intracellular factors, and cellular/tissue environment between the two (Richardson et al., 2022). To our knowledge, intracellular recordings of mechanoreceptor terminals have not been previously reported due to the technical difficulties of accessing the axonal endings with patch-clamp electrodes. Consequently, the functional characteristics of mechanotransduction at the normal physiological site of touch detection remain unknown.

To address this gap in knowledge, we acquired patch-clamp recordings from the afferent terminals of Grandry corpuscles in the bill skin of the tactile specialist Mallard duck (*Anas platyrhynchos domesticus*). The Grandry corpuscle is an avian tactile end-organ innervated by rapidly-adapting mechanoreceptors, which form thin terminals between Schwann cell-derived lamellar cells (Nikolaev et al., 2020; Schneider et al., 2017). The Grandry corpuscle's layered architecture, rapid adaptation, and sensitivity to transient touch make it structurally and functionally analogous to the mammalian Meissner corpuscle (Neubarth et al., 2020; Schwaller et al., 2021; Ziolkowski et al., 2022). Compared to mammals, the high density of corpuscles in the bill of tactile-foraging waterfowl enables persistent electrophysiological investigation of the afferent terminals in these end-organs, the results of which we report here.

**Results and Discussion**

We acquired patch-clamp recordings from the afferent terminal within the Grandry corpuscle using an *ex vivo* bill-skin preparation from late-stage duck embryos (Fig. 1A). Mechanical stimulation of the voltage-clamped afferent terminal revealed fast-inactivating MA current only in response to the dynamic onset (ON) and offset (OFF) phases of the stimulus (Fig. 1B). In current-clamp, both indentation with a probe (Fig. 1C)

58  and current injection (Fig. 1D) caused depolarization of the membrane voltage, which initiated action

59  potentials (APs) in the terminal during both phases. In three corpuscles in which the afferent terminal was

60  patched, simultaneous single-fiber nerve recordings were also established using a section of the same

61  afferent outside of the corpuscle (Fig 1A,E). In these cases, propagating action potentials from the afferent

62  terminal were recorded in the afferent fiber with a one-to-one correlation to APs in the terminal (Fig. 1B-D,

63  bottom). When comparing the responses during the ON and OFF phases, we detected a difference between

64  the rates of current inactivation (Fig. 1F), but not the rates of activation, current-indentation relationship, or

65  AP threshold (Fig. 1E-I). The inactivation rate of MA current in the ON phase ($\tau$ = 8.95 ± 1.82 ms) in the

66  terminal is notably similar to the inactivation rate of fast-inactivating MA current measured from the somas

67  of murine and duck mechanoreceptors *in vitro* (Coste et al., 2010; Schneider et al., 2017; Viatchenko-

68  Karpinski and Gu, 2016). Interestingly, the MA current seen during the OFF phase is a unique response

69  not reported in dissociated neurons or expression systems, even though the OFF response is typical of

70  rapidly adapting mechanoreceptors in *ex vivo* single-fiber recordings. The fast inactivation rate of the OFF

71  response compared to the ON response implies a distinct or modified mechanism of mechanotransduction.

72  This could potentially be dependent on the cellular structure or function of lamellar cells in the corpuscle.

73  As expected, the addition of tetrodotoxin (TTX) to the bill-skin preparation blocked APs and voltage-gated

74  sodium current in the afferent terminal (Fig. 2A-D). In some voltage clamp experiments, mechanical

75  stimulation resulted in large (>1000 pA) depolarizing currents (Fig. 2C) which did not follow the expected

76  current-indentation relationship (Fig. 1H). These currents were blocked by TTX and therefore were voltage-

77  gated sodium currents resulting from brief loss of voltage clamp, likely due to the complex geometry of the
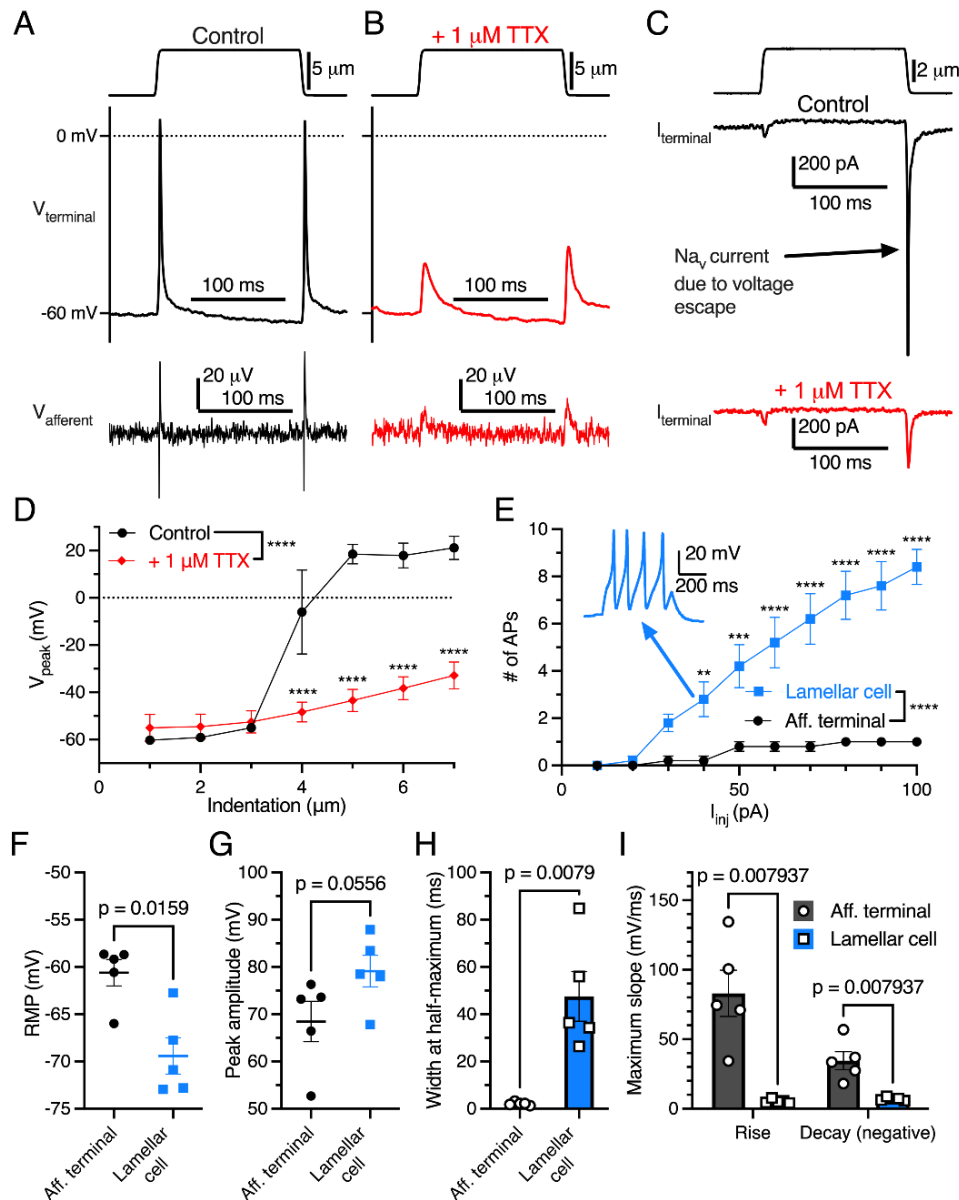
78  afferent.

79  Importantly, APs in the afferent terminal are physiologically distinct from APs fired by Grandry lamellar cells

80  (Fig. 2E-I). Lamellar cell APs are mediated by voltage-gated calcium channels, which are insensitive to TTX

81  (Nikolaev et al., 2020). Lamellar cells fire multiple APs in response to large current injections, whereas the

82  afferent terminal fires a maximum of one AP during the same stimuli (Fig 2E). Additionally, there were

83  significant differences in resting membrane potential, AP width at half-maximum, and maximum slope of

84  rise and decay between the two cell types. These results, along with the single-fiber afferent voltage data

85  which mirrors the terminal voltage (Fig 1B-D), demonstrate that the recordings acquired here are

86  unequivocally from the afferent terminal within the corpuscle.

87  Here, we have shown that mechanical stimulation evokes MA current in the afferent terminal which initiates

88  propagating APs. Critically, MA current in the terminal has properties closely resembling those observed in

89  dissociated neuron somas. This ultimately confirms the validity of using *in vitro* models to study

90  mechanotransducers. At the same time, an important aspect of the afferent terminal response *in situ* is

91  absent from cultured cells: the MA current in the OFF phase. Further studies of rapidly adapting corpuscles

92  and other mechanoreceptor endings will be required to understand the mechanism underlying the OFF

93    response. Together, these findings reveal fundamental characteristics of mechanotransduction at the

94    physiological site of touch detection in mechanosensory neurons.
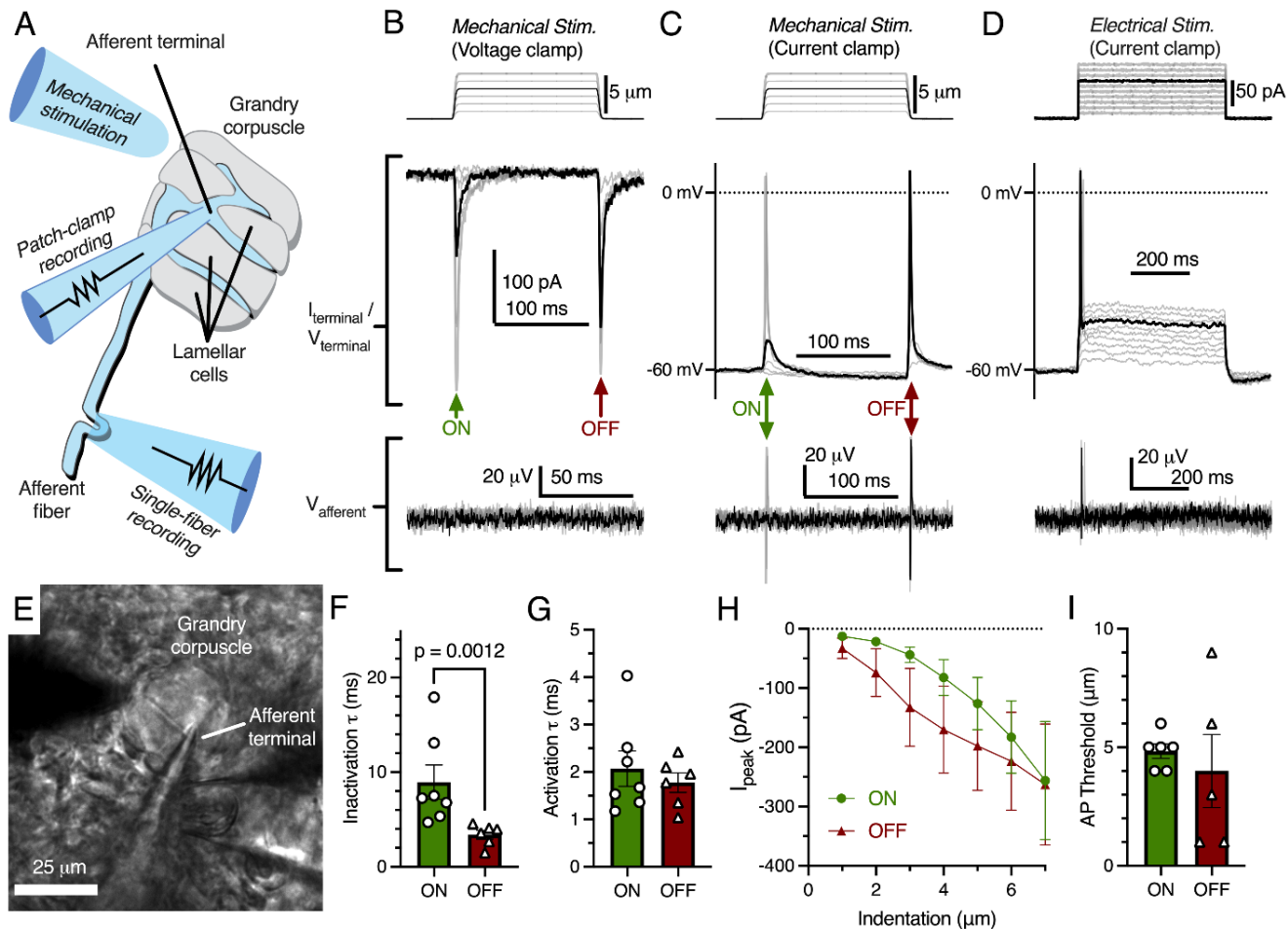


**Figure 1. Mechanotransduction in the terminal afferent of Grandry corpuscle. (A)** Illustrated representation of the experimental setup. **(B)** The mechanical step stimulus applied with a glass probe (top), representative MA current responses in the terminal while voltage-clamped at -60 mV (middle), and simultaneous extracellular voltage signal from the connected afferent (bottom). **(C)** The mechanical stimulus (top), voltage responses and APs in the terminal in current-clamp (middle), and APs measured further along the afferent (bottom). **(D)** The current injection stimulus (top), voltage responses and action potentials in the terminal in current-clamp (middle), and APs measured in the afferent (bottom). **(E)** Example bright-field image of the experimental setup. **(F)** Quantification of the kinetics of MA current inactivation, **(G)** activation, **(H)** peak MA current-indentation relationship (n = 7/6 for ON/OFF, respectively), and **(I)** AP threshold measured in the dynamic onset phase the stimulus (ON) and the dynamic offset phase of the stimulus (OFF). Only the difference in inactivation $\tau$ between the ON and OFF phase was statistically significant (p < 0.05). Statistics: Mann-Whitney U test (F,G,I) or two-way ANOVA (H). Symbols indicate data from individual cells. Data in F-I were obtained from at least 3 independent skin preparations, and shown as mean ± SEM.

**Figure 2. Electrogenic events in mechanoreceptor terminal and lamellar cells are carried out by different mechanisms. (A)** A suprathreshold mechanical stimulus (top), APs in the terminal (middle), and propagated APs from the connected afferent (bottom). **(B)** A suprathreshold mechanical stimulus applied in 1 $\mu$M TTX (top), AP-absent voltage responses in the terminal in current-clamp (middle), and extracellular receptor potentials in the afferent (bottom). **(C)** A suprathreshold mechanical stimulus (top), current responses in the terminal while voltage-clamped at -60 mV without 1 $\mu$M TTX (middle), and with 1 $\mu$M TTX (bottom). **(D)** Voltage-indentation relationship in the absence or presence of 1 $\mu$M TTX (n = 5 for both groups). **(E)** The number of APs from increasing current injections in lamellar cells and afferent terminals (n = 5 for both groups). **(F)** Resting membrane potential (RMP), **(G)** peak AP amplitude, **(H)** AP width at the half-maximum, and **(I)** the maximum slope of the AP rise or decay in the afferent terminal versus lamellar cells of the corpuscle. The AP-current injection relationship, resting membrane potential, width at half-maximum, max rise slope, and max decay slope were significantly different between terminal afferent and lamellar cells (p < 0.05). Statistics: Mann-Whitney U test (F-I) or two-way ANOVA with Holm-Sidak post-hoc test (D,E). **P=0.0084, ***P=0.0004, ****P<0.0001. Symbols indicate data from individual cells. Data in D-I were obtained from at least 3 independent skin preparations, and shown as mean ± SEM.

6

**Supplemental Figure Legends**

**Figure 1 – Source Data 1. Original data for Figure 1F-I**

**Figure 2 – Source Data 2. Original data for Figure 2D-I**

**Materials and Methods**

*Ex vivo* **bill-skin preparation.** Experiments with duck embryos (*Anas platyrhynchos domesticus*) were approved by and performed in accordance with guidelines of the Institutional Animal Case and Use Committee of Yale University, protocol 11526. Bill preparation was slightly modified from previously published methods (Nikolaev et al., 2020). Intact skin was carefully removed from the bill of duck embryos (aged embryonic day 25 to 27, sex not determined) using a sharp scalpel tip in ice-cold L-15 media. The bill-skin was placed upside-down (epidermis on bottom) in the recording chamber under a slice anchor. Corpuscles and afferents in the dermis were visualized on an Olympus BX51WI upright microscope with an ORCA-Flash 4.0 LT camera (Hamamatsu). At room temperature (22-23°C), the bill-skin preparation was treated for 5 minutes with 2 mg/mL collagenase P (Roche) in Krebs solution containing (in mM) 117 NaCl, 3.5 KCl, 2.5 $CaCl_2$, 1.2 $MgCl_2$, 1.2 $NaH_2PO_4$, 25 $NaHCO_3$, and 11 glucose, saturated with 95% $O_2$ and 5% $CO_2$ (pH = 7.3-7.4), then washed with fresh Krebs solution.

**Patch-clamp electrophysiology.** Recordings were at room temperature using a MultiClamp 700B amplifier, Digidata 1550A digitizer, and pClamp 10 software (Molecular Devices). Standard-wall, 1.5 mm diameter borosilicate pipettes with tip resistances of 2-5 MΩ were pulled using a P-1000 micropipette puller (Sutter Instruments). Pipettes were filled intracellular solution containing (in mM) 135 K-gluconate, 5 KCl, 0.5 $CaCl_2$, 2 $MgCl_2$, 5 EGTA, 5 HEPES, 5 $Na_2ATP$, and 0.5 $Na_2GTP$ (pH 7.3 with KOH). All experiments were performed in Krebs solution at room temperature. Data were sampled at 20 kHz and low-pass filtered at 2 kHz. Terminals were recorded in whole-cell mode and were held at -60 mV during voltage-clamp experiments. Resting membrane potential was measured in current-clamp mode shortly after breaking in. In both voltage- and current-clamp, mechanical stimuli were applied to a single corpuscle using a blunt glass probe (2 to 10 μm tip diameter) mounted on a piezoelectric-driven actuator (Physik Instrumente GmbH. A mechanical step stimulus was applied to corpuscles starting at 1 μm and increasing by 1 μm after each indentation. The static plateau of the step stimulus lasted 150 ms, while the ramp had a duration of 3 ms for both the ON and OFF phases. For both phases in each terminal, the inactivation rate (τ) of the MA current was calculated by fitting the equation $I = I_0*exp^{(-t/\tau)}$ to the decaying portion of the largest three MA current responses, and averaging those τ values. The activation τ was calculated similarly using the rise portion of the response. The threshold was measured in current-clamp as the smallest indentation which elicited an AP. In current-clamp, depolarizing current steps (from 10 to 100 pA in 10 pA increments) were applied to elicit APs in the afferent terminal and lamellar cells. The first AP in these recordings was used to calculate the peak amplitude, width at half-maximum and maximum slope of rise and decay for the terminal versus lamellar cells. Experiments were not corrected for liquid-junction potential.

159 **Single-fiber recording.** Recordings from single afferent fibers of corpuscles were acquired simultaneously

160 with patch-clamp recordings for three corpuscles, using the second channel of the MultiClamp 700B

161 amplifier. Single-fiber recording pipettes were created pulled from thin-wall, 1.5 mm diameter borosilicate

162 glass capillaries using a P-1000 micropipette puller (Sutter Instruments) to create tip diameters of 5 to 30

163 $\mu$m, then filled with Krebs solution. Pipettes were placed on an electrode headstage connected to a High

164 Speed Pressure Clamp (ALA Scientific Instruments). Light (1 to 20 mmHg) positive pressure was applied

165 from the recording electrode to clear away tissue from a corpuscle-associated afferent. Negative pressure

166 was then applied until a large section (~5 $\mu$m) of the afferent was sucked into the pipette. Extracellular

167 afferent voltage was recording in current-clamp mode, sampled at 20 kHz and low-pass filtered at 1 kHz.

168 **Data analysis.** Data from afferent terminals and lamellar cells were acquired from separate, individual

169 preparations from different animals. Data were analyzed and plotted in GraphPad Prism 9.4.1 (GraphPad

170 Software, LLC) as individual data points or means ± SEM, unless otherwise indicated.

## Acknowledgements

## Competing interests

177 The authors declare no competing interests.

## References

179 Buchholtz LJ von, Ghitani N, Lam RM, Licholai JA, Chesler AT, Ryba NJP. 2021. Decoding cellular
180     mechanisms for mechanosensory discrimination. *Neuron* **109**:285-298.e5.
181     doi:10.1016/j.neuron.2020.10.028
182 Chesler AT, Szczot M, Bharucha-Goebel D, Čeko M, Donkervoort S, Laubacher C, Hayes LH, Alter K,
183     Zampieri C, Stanley C, Innes AM, Mah JK, Grosmann CM, Bradley N, Nguyen D, Foley AR, Le
184     Pichon CE, Bönnemann CG. 2016. The Role of PIEZO2 in Human Mechanosensation. *N Engl J*
185     *Med* **375**:1355–1364. doi:10.1056/NEJMoa1602812
186 Coste B, Mathur J, Schmidt M, Earley TJ, Ranade S, Petrus MJ, Dubin AE, Patapoutian A. 2010. Piezo1
187     and Piezo2 are essential components of distinct mechanically-activated cation channels. *Science*
188     **330**:55–60. doi:10.1126/science.1193270
189 Handler A, Ginty DD. 2021. The mechanosensory neurons of touch and their mechanisms of activation.
190     *Nat Rev Neurosci* **22**:1–17. doi:10.1038/s41583-021-00489-x
191 Lewis AH, Cui AF, McDonald MF, Grandl J. 2017. Transduction of repetitive mechanical stimuli by Piezo1
192     and Piezo2 ion channels. *Cell Rep* **19**:2572–2585. doi:10.1016/j.celrep.2017.05.079
193 Loewenstein WR, Rathkamp R, With the Assistance of I. Zamudio. 1958. The sites for mechano-electric
194     conversion in a Pacinian corpuscle. *Journal of General Physiology* **41**:1245–1265.
195     doi:10.1085/jgp.41.6.1245
196 Neubarth NL, Emanuel AJ, Liu Y, Springel MW, Handler A, Zhang Q, Lehnert BP, Guo C, Orefice LL,
197     Abdelaziz A, DeLisle MM, Iskols M, Rhyins J, Kim SJ, Cattel SJ, Regehr W, Harvey CD,

198    Drugowitsch J, Ginty DD. 2020. Meissner corpuscles and their spatially intermingled afferents
199        underlie gentle touch perception. *Science* **368**:eabb2751. doi:10.1126/science.abb2751
200 Nikolaev YA, Feketa VV, Anderson EO, Schneider ER, Gracheva EO, Bagriantsev SN. 2020. Lamellar
201        cells in Pacinian and Meissner corpuscles are touch sensors. *Sci Adv* **6**:abe6393.
202        doi:10.1126/sciadv.abe6393
203 Ranade SS, Woo S-H, Dubin AE, Moshourab RA, Wetzel C, Petrus M, Mathur J, Bégay V, Coste B,
204        Mainquist J, Wilson AJ, Francisco AG, Reddy K, Qiu Z, Wood JN, Lewin GR, Patapoutian A.
205        2014. Piezo2 is the major transducer of mechanical forces for touch sensation in mice. *Nature*
206        **516**:121–125. doi:10.1038/nature13980
207 Richardson J, Kotevski A, Poole K. 2022. From stretch to deflection: the importance of context in the
208        activation of mammalian, mechanically activated ion channels. *FEBS J* **289**:4447–4469.
209        doi:10.1111/febs.16041
210 Schneider ER, Anderson EO, Mastrotto M, Matson JD, Schulz VP, Gallagher PG, LaMotte RH, Gracheva
211        EO, Bagriantsev SN. 2017. Molecular basis of tactile specialization in the duck bill. *Proc Natl*
212        *Acad Sci U S A* **114**:13036–13041. doi:10.1073/pnas.1708793114
213 Schwaller F, Bégay V, García-García G, Taberner FJ, Moshourab R, McDonald B, Docter T, Kühnemund
214        J, Ojeda-Alonso J, Paricio-Montesinos R, Lechner SG, Poulet JFA, Millan JM, Lewin GR. 2021.
215        USH2A is a Meissner's corpuscle protein necessary for normal vibration sensing in mice and
216        humans. *Nat Neurosci* **24**:74–81. doi:10.1038/s41593-020-00751-y
217 Viatchenko-Karpinski V, Gu JG. 2016. Mechanical sensitivity and electrophysiological properties of
218        acutely dissociated dorsal root ganglion neurons of rats. *Neurosci Lett* **634**:70–75.
219        doi:10.1016/j.neulet.2016.10.011
220 Wang L, Zhou H, Zhang M, Liu W, Deng T, Zhao Q, Li Y, Lei J, Li X, Xiao B. 2019. Structure and
221        mechanogating of the mammalian tactile channel PIEZO2. *Nature* **573**:225–229.
222        doi:10.1038/s41586-019-1505-8
223 Zheng W, Nikolaev YA, Gracheva EO, Bagriantsev SN. 2019. Piezo2 integrates mechanical and thermal
224        cues in vertebrate mechanoreceptors. *Proc Natl Acad Sci U S A* **116**:17547–17555.
225        doi:10.1073/pnas.1910213116
226 Ziolkowski LH, Gracheva EO, Bagriantsev SN. 2022. Tactile sensation in birds: Physiological insights
227        from avian mechanoreceptors. *Current Opinion in Neurobiology* **74**:102548.
228        doi:10.1016/j.conb.2022.102548
229

**B** *Mechanical Stim.* (Voltage clamp)

**C** *Mechanical Stim.* (Current clamp)

**D** *Electrical Stim.* (Current clamp)

5 μm

5 μm

50 pA

0 mV

0 mV

100 pA
100 ms

200 ms

$I_{terminal}$ /
$V_{terminal}$

100 ms

-60 mV

-60 mV

ON

OFF

ON

OFF

$V_{afferent}$

20 μV   50 ms

20 μV   100 ms

20 μV   200 ms

**A**
Afferent terminal
Mechanical stimulation
Grandry corpuscle
Patch-clamp recording
Lamellar cells
Afferent fiber
Single-fiber recording

**E**
Grandry corpuscle
Afferent terminal
25 μm

**F**
Inactivation τ (ms)
p = 0.0012
ON    OFF

**G**
Activation τ (ms)
ON    OFF

**H**
$I_{peak}$ (pA)
Indentation (μm)
ON
OFF

**I**
AP Threshold (μm)
ON    OFF

**A** Control

5 μm

**B** + 1 μM TTX

5 μm

**C**

$I_{terminal}$

2 μm

Control

200 pA
100 ms

$Na_V$ current due to voltage escape

0 mV

$V_{terminal}$

-60 mV

100 ms

100 ms

+ 1 μM TTX

$I_{terminal}$

200 pA
100 ms

$V_{afferent}$

20 μV
100 ms

20 μV
100 ms

**D**

$V_{peak}$ (mV)

● Control
◆ + 1 μM TTX

****

**** **** **** ****

Indentation (μm)

**E**

# of APs

20 mV
200 ms

■ Lamellar cell
● Aff. terminal

** *** **** **** **** **** ****

****

$I_{inj}$ (pA)

**F**

RMP (mV)

p = 0.0159

Aff. terminal    Lamellar cell

**G**

Peak amplitude (mV)

p = 0.0556

Aff. terminal    Lamellar cell

**H**

Width at half-maximum (ms)

p = 0.0079

Aff. terminal    Lamellar cell

**I**

Maximum slope (mV/ms)

◉ Aff. terminal
▣ Lamellar cell

p = 0.007937

p = 0.007937

Rise    Decay (negative)